Supporting Material
3D Traction stresses activate protease-dependent invasion of cancer cells
Aung et al.,

Effect Of Cell Dissolving Solution On Matrigel Network

The effect of the cell removal process on swelling and/or shrinking of the Matrigel network was determined by comparing the confocal image stacks of the Matrigel network embedded with fluorescent beads before and after exposure to cell dissolving solution. Here we used acellular Matrigel networks. As evidenced from the confocal images and the displacement field analyses no significant changes in the network due to the cell dissolving solution was observed (Fig. S2B-E).

Characterization Of Matrigel Networks

Prior to characterization, the Matrigels were incubated overnight in growth medium (GM) at 37° C and 5% CO_2. Surface topography of Matrigels of T = 30 and 10 μm tethered to a glass-bottom culture dish was obtained in GM using a Bioscope Atomic Force Microscope (BAFM) equipped with a Nanoscope IIIA controller (Bruker). The topographical images were obtained in contact mode by using Si_3N_4 cantilevers with 0.02 N/m nominal spring constants at forces of ~ 4 nN over areas of 10×10 μm^2. The surface roughness values were determined using the Nanoscope software and the images were processed with a flattening order of 2 to account for tilts during the measurements. The measurements show similar roughness and topography for the Matrigel networks of 10 and 30 μm thickness (Fig. S4A, B).

To determine the elastic modulus, borosilicate glass beads of 2 μm diameter attached to tipless cantilevers with 0.06 N/m nominal spring constants (Novascan Technologies, IA) were used to indent several regions of 30-μm-thick Matrigels tethered to a glass bottom dish and equilibrated in GM. The trigger threshold and the ramp size during the measurements were set as 30 nm and 1.8 μm, respectively. The maximum indentation depth did not exceed 2 μm during the measurements. The spring constant of the cantilever was verified using a beam shaped cantilever with 0.16 N/m calibrated spring constant (Bruker). Photodetector sensitivity was determined by obtaining force curves on a freshly cleaved mica surface. Representative force curves for loading and unloading are shown in Fig. S4C, showing no hysteresis. The curves were fitted to the Hertzian model corrected for finite thickness using a custom Matlab code to calculate the elastic modulus. The Matrigel network was found to have an elastic modulus of ~ 400 Pa (Fig. S4D) (1).

Mechanical Yielding Tests of Matrigel Networks

Glass-bottom dishes with grid markings were generated by attaching Cellattice sheets (Electron Microscopy Sciences) underneath the dishes using an optical adhesive. The glass surface within the dish was activated and the Matrigel networks embedded with fluorescent beads were synthesized as described above. Specific locations of the Matrigel network and the lattice grids were imaged at 60x magnification by using a water immersion lens mounted onto a spinning disk Confocal. 10-μm thick image stacks of the network with embedded fluorescent beads were obtained at vertical increments of 0.2 μm. A schematic of the experimental procedure to measure the mechanical yielding of the matrix is outlined in Fig. S7. The tips of cantilevers with a spring constant of 0.5 N/m were modified by attaching 30 μm diameter glass beads. These modified tips

were mounted onto the BAFM and used to indent the Matrigel at the imaged locations. One set of deflection threshold was used to indent 5 different locations before increasing the threshold to apply larger forces. The deflection threshold ranged from 10 to 70 nm while ramp sizes for all indentations were set at 1.872 μm. The indentation depth, defined as the difference between the cantilever deflection and the z ramp displacement obtained from the force curves, was used to calculate the maximum applied compressive pressure using the Hertzian model corrected for finite substrate thickness (1). These locations were then re-imaged using the spinning disk confocal microscope as mentioned above. The image stacks obtained before and after the BAFM indentation were processed to account for rotational and translation shifts using custom MATLAB software. Specifically, maximum cross correlation between the pre-indentation images and the rotated post-indentation images was determined to correct for the rotational and translational shifts. The displacement field was obtained from corrected image stacks using 3D image correlation algorithms described elsewhere (2).

Results Of Mechanical Yielding Of The Matrigel Network. Our PIV analyses for the displacement fields show an absence of permanent deformation of the Matrigel network exposed to a compressive pressure of 207.4Pa (Fig. S8A,B). This was further confirmed by confocal imaging of the Matrigel networks embedded with beads, which shows identical images before and after the indentation (Fig. S8B).

Secreted Protease Activity Detection Using Zymography

To obtain ~ 30 μm thick gels, 7 μL of the thawed Matrigel solution was added into each well of a 24-well plate. The Matrigel solution was spread across the well using a pipette at 4° C and left for 10 minutes before transferring to 37° C for 30 minutes. PBS was added to the wells containing Matrigel networks and the entire plate was sterilized by exposing to UV for 30 minutes. The PBS was replaced with OM and incubated overnight at 37^{o}C before plating the cells. The OM was removed and the cells were plated at a density of 10,000 cells/cm^{2} in 650 μL OM for each well, and cell invasion into Matrigel was allowed to persist for 6 hours resulting in a ϕ_{3D} >20° (Fig. S11A). 600 μL of the collected OM was centrifuged to remove non-adhered cells at 1,000 RPM for 10 minutes. 500 μL of this solution was concentrated for secreted factors by using centrifugal filter tubes with a molecular weight cutoff of 50 kDa (Microcon) as instructed by the manufacturer's protocol. Conditioned medium from 8 wells were collected to obtain a concentrated solution of ~ 30 μL.

The concentrated conditioned medium was assayed for protease activity as described elsewhere (3). Briefly, we used a stacking gel comprised of 3.68 % acrylamide and 0.01 % bisacrylamide and a resolving gel comprised of 7.5 % acrylamide gel, 0.33 % bisacrylamide, and 0.08% gelatin. After the gels were polymerized, cathode and anode reservoir buffers were added to the outer and inner chamber of an upright electrophoresis apparatus, respectively. The cathode buffer consisted of 10.25 mM ammediol, 10 mM glycine, and 0.1 % SDS adjusted to pH of 9.39 while anode buffer consisted of 21 mM ammediol adjusted to pH of 8.23. The gel lanes consisted of a positive control, a negative control, concentrated conditioned medium, activated concentrated conditioned medium, and control for activated concentrated conditioned medium. The positive and negative controls consisted of 0.1 μg of Bovine Collagenase IV (Gibco) and OM concentrated from 8 wells containing acellular Matrigels, respectively. To activate the concentrated conditioned medium, the medium was incubated in 1 mM 4-Aminophenylmercuric

Acetate (APMA, Sigma-Aldrich) dissolved in 80 mM NaOH for 2 hours in 37°C prior to loading the samples. The control for the activated and concentrated conditioned medium was generated by incubating the medium in 80mM NaOH without APMA. 16 μL of each solution was loaded into their respective lanes and gel electrophoresis was run for 1.5 hours using a voltage of 150 V. After electrophoresis, the proteins in each lane were renatured by submerging the gel in a developing buffer mixed with 2.5 % Triton-X 100 for one hour with frequent washing before incubating the gels in developing buffer overnight at 37 °C. The developing buffer used consisted of 50 mM Tris base, 200 mM NaCl, 5.2 μM $ZnCl_2$, 5 mM $CaCl_2 \cdot 2H_2O$, and 3 mM NaN_3. After the overnight incubation, the gel was stained for 30 minutes in 0.125 % Coomassie brilliant blue R-250 dissolved in a mixture of methanol, acetic acid, and water at volume ratios of 1.25:0.5:0.75. The gel was subsequently destained in a solution comprised of methanol, water, and formic acid at a volume ratio of 1.5:3.5:0.05. The gel was destained until the desired contrast between the light bands devoid of gelatin due to protease-mediated degradation and the surrounding gelatin was achieved. The gel was frequently imaged to document the contrast.

The presence of bands in the lane consisting of concentrated conditioned medium indicates that secreted proteases were present within the medium. The finding that the bands did not shift when compared to the lane consisting of medium treated with APMA further reveals that the secreted proteases were in the active form (Fig. S11B).

Secreted Protease Activity Detection Using Fluorogenic Peptides

Matrigels were synthesized in 24-well plates as previously mentioned. Cells were plated onto the Matrigel-containing wells at a density of 6,000 cells/cm^2 with a total volume of 500 μL. Acellular Matrigel cultured in GM under identical culture conditions was used as a negative control (NC). The cells were allowed to invade into the Matrigel for 3 hours ($\phi_{3D} > 15°$) before collecting 200 μL of the media from each well. For each well, the collected media was centrifuged to remove any suspended cells. 98 μL of the collected media was then mixed with 2 μL of 0.5 mM stock solution of MMP sensitive fluorogenic peptide substrate (Cat # ES001 & Lot # DHY08, R&D Systems). This approach was used to circumvent the interference from Matrigel during the measurements from the plate reader. For the positive control, 0.1 μg of Bovine Collagenase IV solubilized in 98 μL of PBS was mixed with 2 μL of the peptide substrate stock. The mixtures were transferred to a 96 well plate and allowed to incubate for 15 minutes at 37° C. The fluorescence caused by MMP cleavage was determined using a plate reader (Infinite 200 Pro, Tecan) at excitation and emission wavelengths of 320 ± 4.5 and 405 ± 10 nm, respectively. The higher fluorescence value for conditioned medium from invading MDA-MB-231 cells compared to NC indicates higher protease activity associated with the invasion of MDA-MB-231 cells (Fig. 3C).

Supplementary Figures

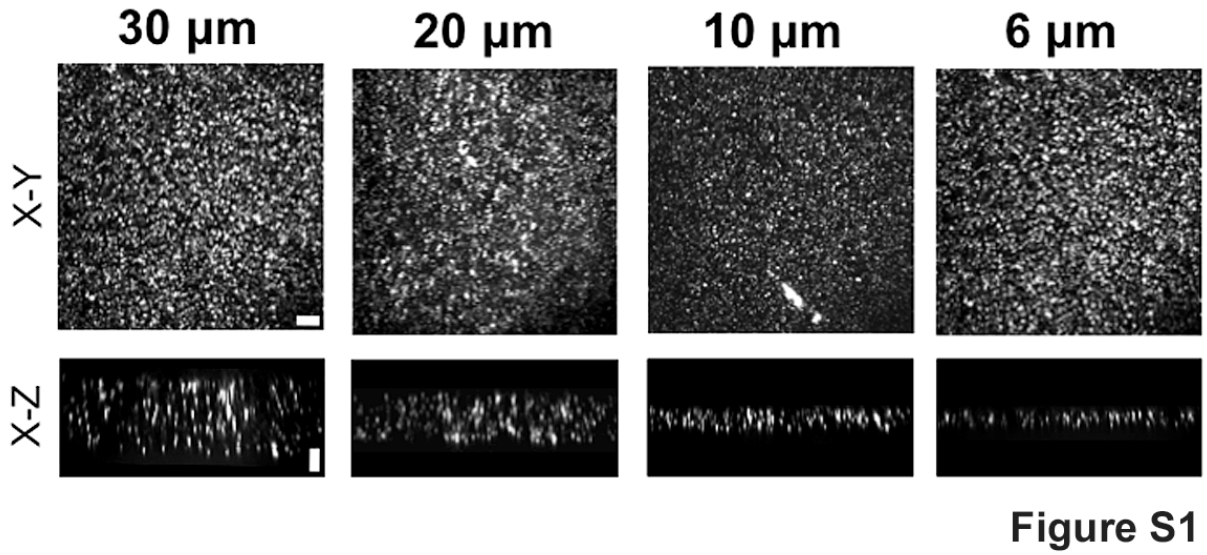

Figure S1: Verification of Matrigel network thickness. X-Y and X-Z planes of Matrigel networks created with varying thickness and tethered to glass obtained via confocal imaging. Horizontal and vertical scale bars represent 10 µm.

A

[NH_4OH]	pH
5 mM	8.4
10 mM	9.6
20 mM	10.1

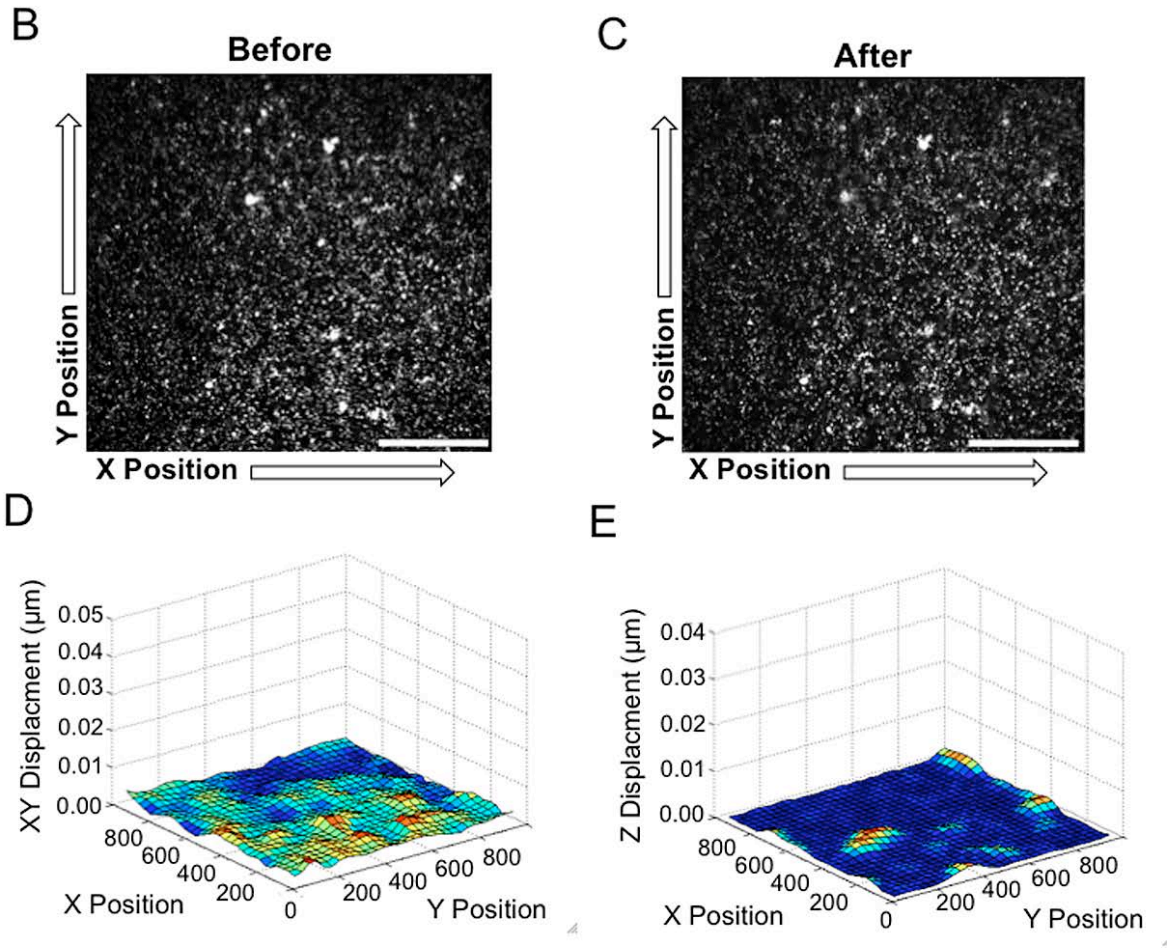

Figure S2

Figure S2: Effect of cell dissolving solution on the Matrigel network. (A) Table shows the pH of the cell dissolving solution containing 3% Triton-X 100 with increasing concentration of NH_4OH. Confocal images of the surface of the Matrigel network embedded with fluorescent beads (B) before and (C) after the treatment with the dissolving solution comprised of 20 mM NH_4OH and 3% Triton-X 100. The tangential (D) and the vertical (E) displacement fields obtained by image correlation analysis show that the effect of dissolving solution on Matrigel network is negligible. Scale bars: 30 µm.

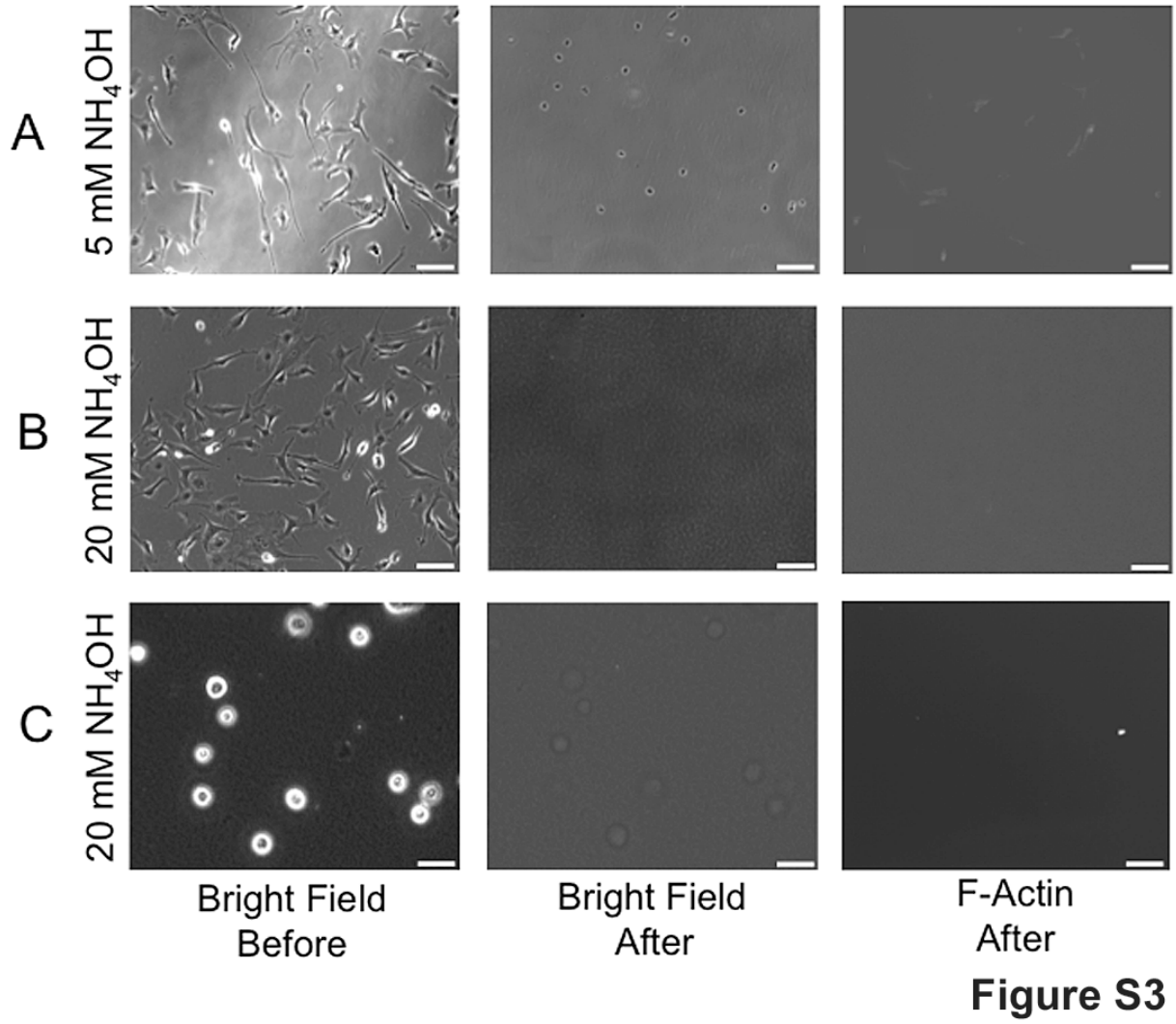

Figure S3: Efficiency of cell removal. MDA-MB-231 cells on Petri dishes were treated with cell dissolving solution containing 3% Triton-X 100 and (A) 5 mM and (B) 20 mM NH_4OH. (C) MDA-MB-231 cells invading into 30 μm thick Matrigels were treated with cell dissolving solution containing 20 mM NH_4OH and 3% Triton-X 100. Bright field images of cells were taken before (left column) and 15 minutes after (right column) the treatment with cell dissolving solution. F-Actin staining validates that 20 mM NH_4OH and 3% Triton-X 100 is sufficient to remove the cells (right column). Scale bars: 50 μm.

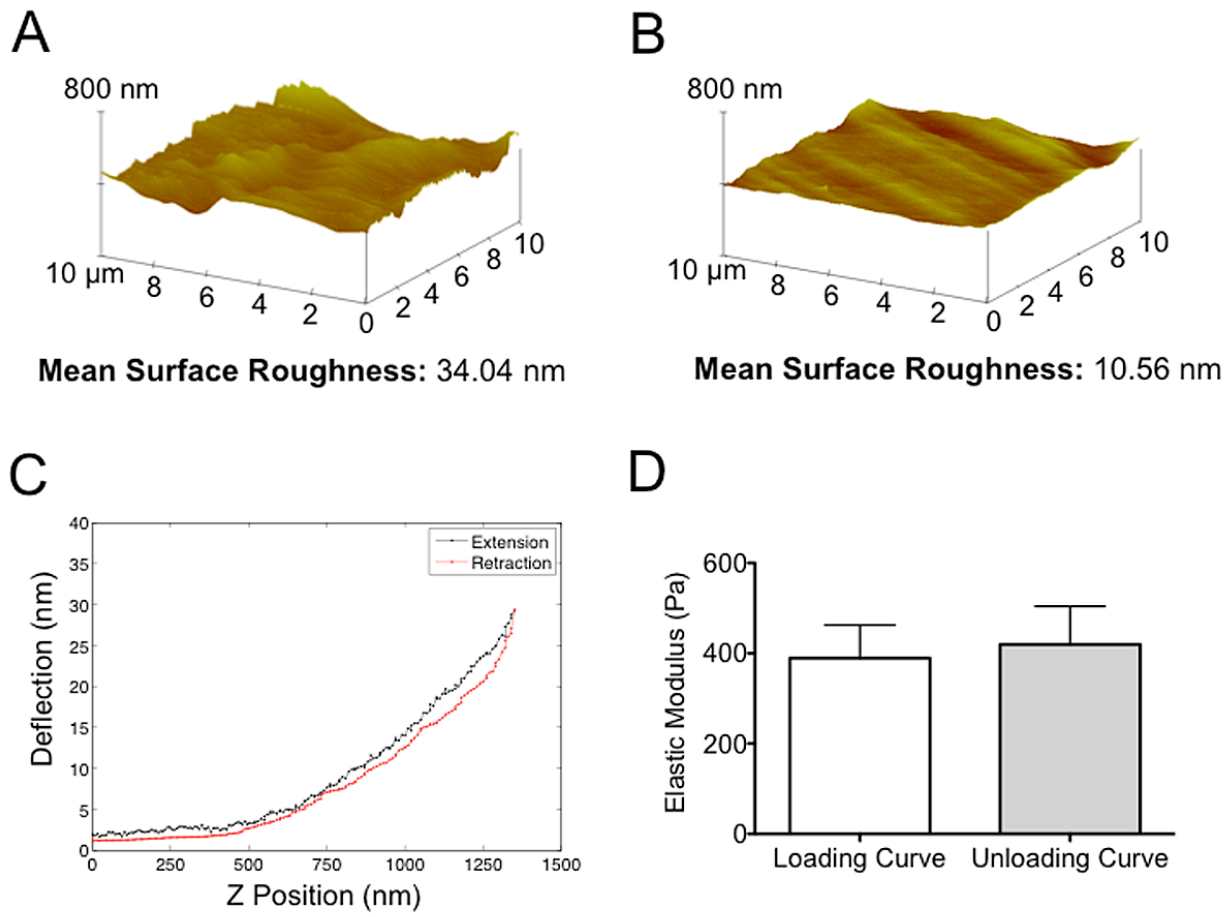

Figure S4

Figure S4: Characterization of Matrigel networks tethered to glass. Surface topography and roughness of 30 µm (A) and 10 µm (B) thick Matrigel networks tethered to glass were obtained by using a BAFM. (C) The elastic modulus of the 30 µm thick Matrigel estimated from the indentation of several locations of the equilibrated Matrigel. The Hertzian model corrected for finite thickness was fitted to the approach and retraction curves to obtain the elastic modulus of the Matrigel network.

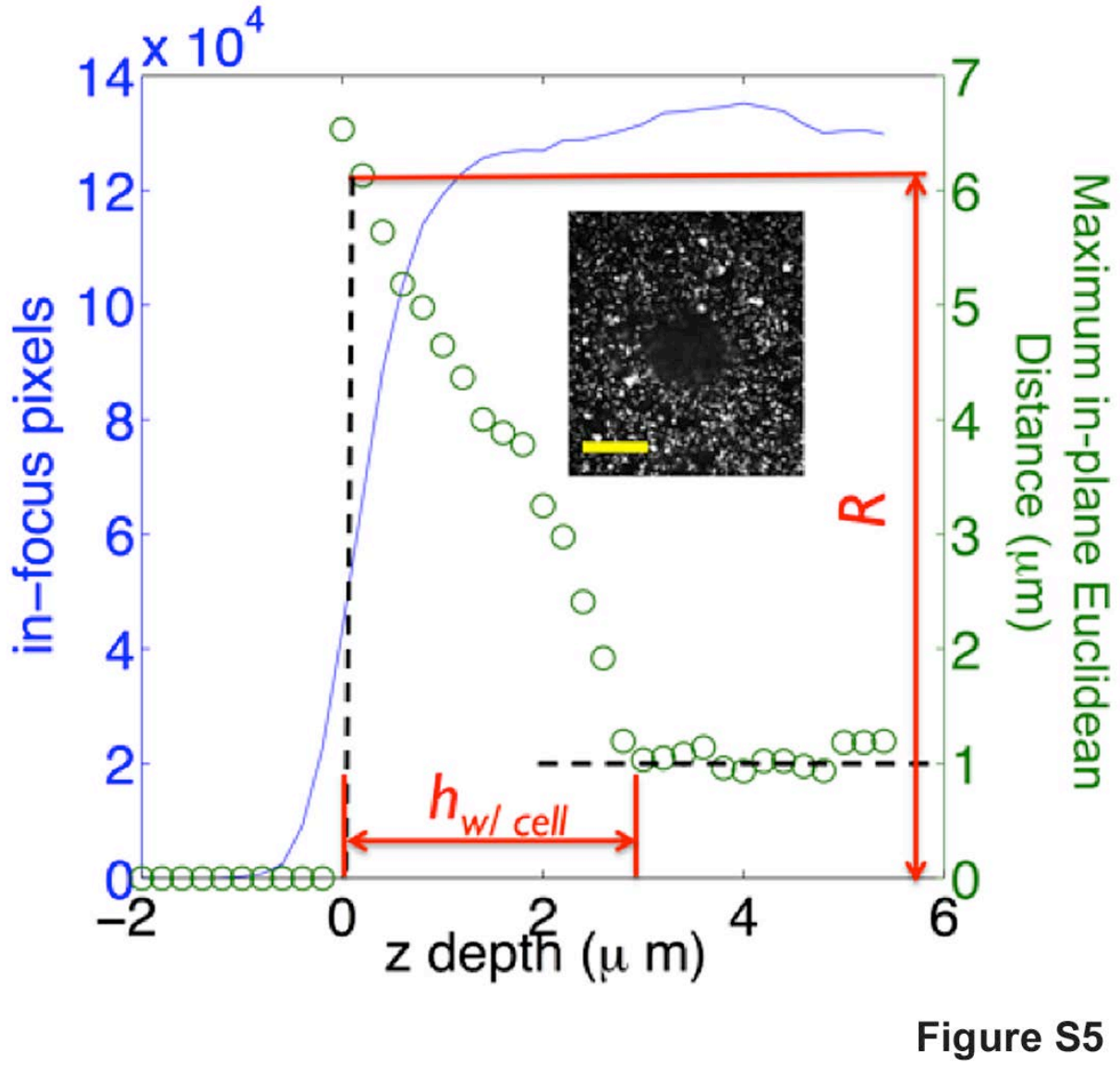

Figure S5. Quantification of the matrix indentation profile caused by the invading cells from confocal images. Image analysis of a confocal fluorescent bead z-stack of a Matrigel network embedded with fluorescent beads that has been indented by an invading cell (see inset, scale bar = 5 microns). The indentation appears as a dark region of out-of focus beads that have been displaced downwards by the cell. Blue line (left y-axis): Number of in-focus pixels in each z-slice as a function of z. The z-position with highest variation of in-focus pixels corresponds to the top surface of the network. Green circles (right y-axis): Maximum Euclidean distance to an in-focus pixel in each z-slice as a function of z. The maximum value of the Euclidean distance in the whole Matrigel was defined as *R*. The *z*-slice at which the Euclidean distance reached its floor was designated as the bottom of the cell. The z-distance between the top and bottom slices allows to determine $h_{w/\,cell}$.

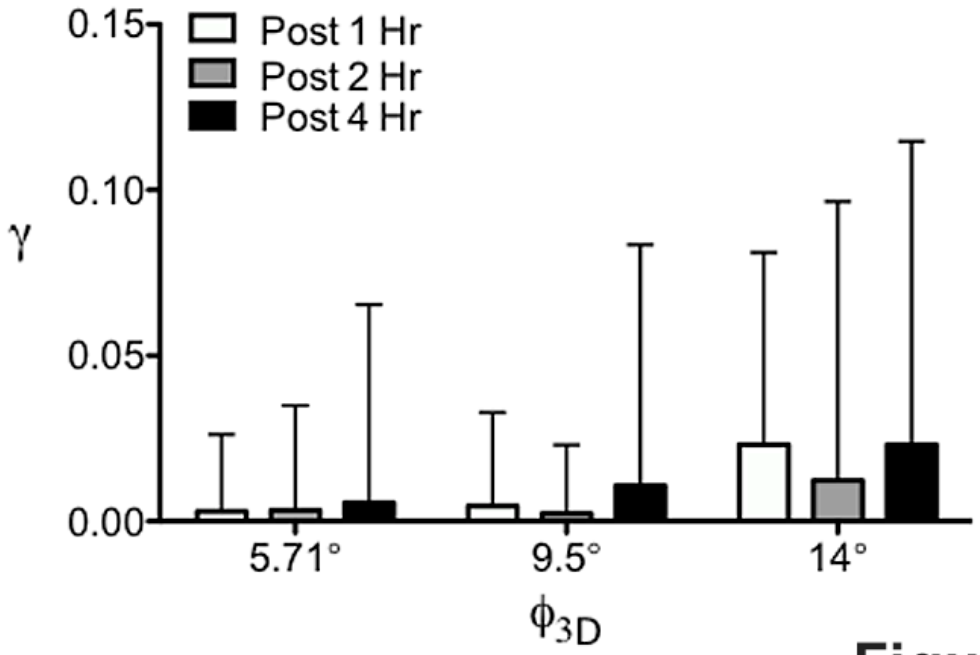

Figure S6

Figure S6: Effect of time on degree of permanent deformation. Graph of the extent of permanent matrix deformation, γ, at different ϕ_{3D}, where the cells were allowed to invade into 30 μm thick Matrigel for 1, 2, and 4 hours, rules out the influence of time on γ. The plot was generated by binning the cell population around the listed angles with an allowance of $\pm 1°$.

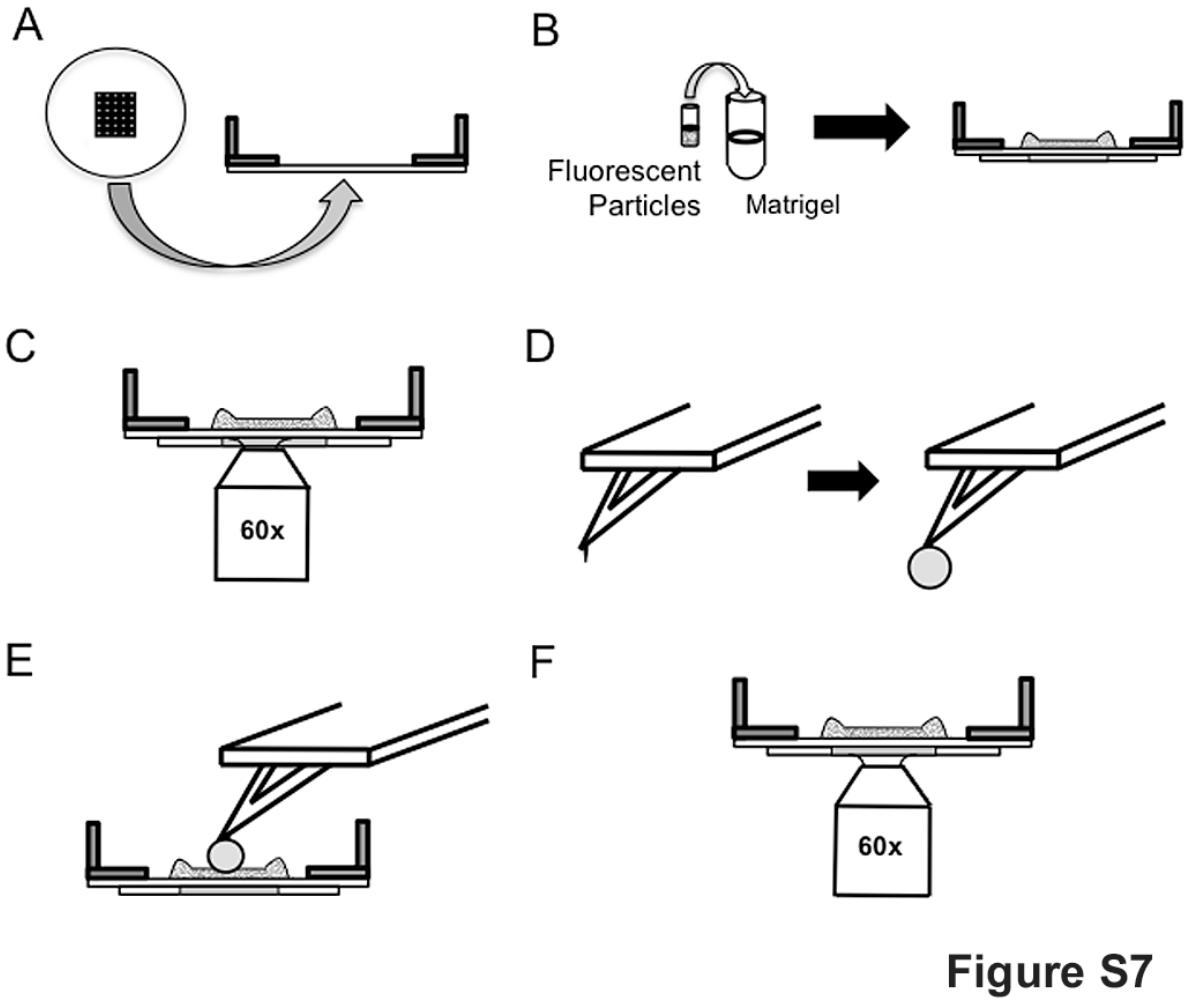

Figure S7: Schematic representation of the experiments utilized to determine the mechanical yielding of the Matrigel in the absence of cells. (A) Cell lattice grid attached to glass-bottom dish. (B) Matrigel network embedded with fluorescent beads tethered to the glass-bottom dish. (C) Confocal microscope was used to acquire Z-stack images of the fluorescent beads at specific grid locations. (D) AFM cantilever tip modified with 30 μm diameter glass bead. (E) The modified cantilever was subsequently used to indent the pre-imaged locations of the Matrigel network using BAFM. (F) Re-imaging of the above locations (imaged in E) to determine permanent deformation of the Matrigel due to mechanical loading.

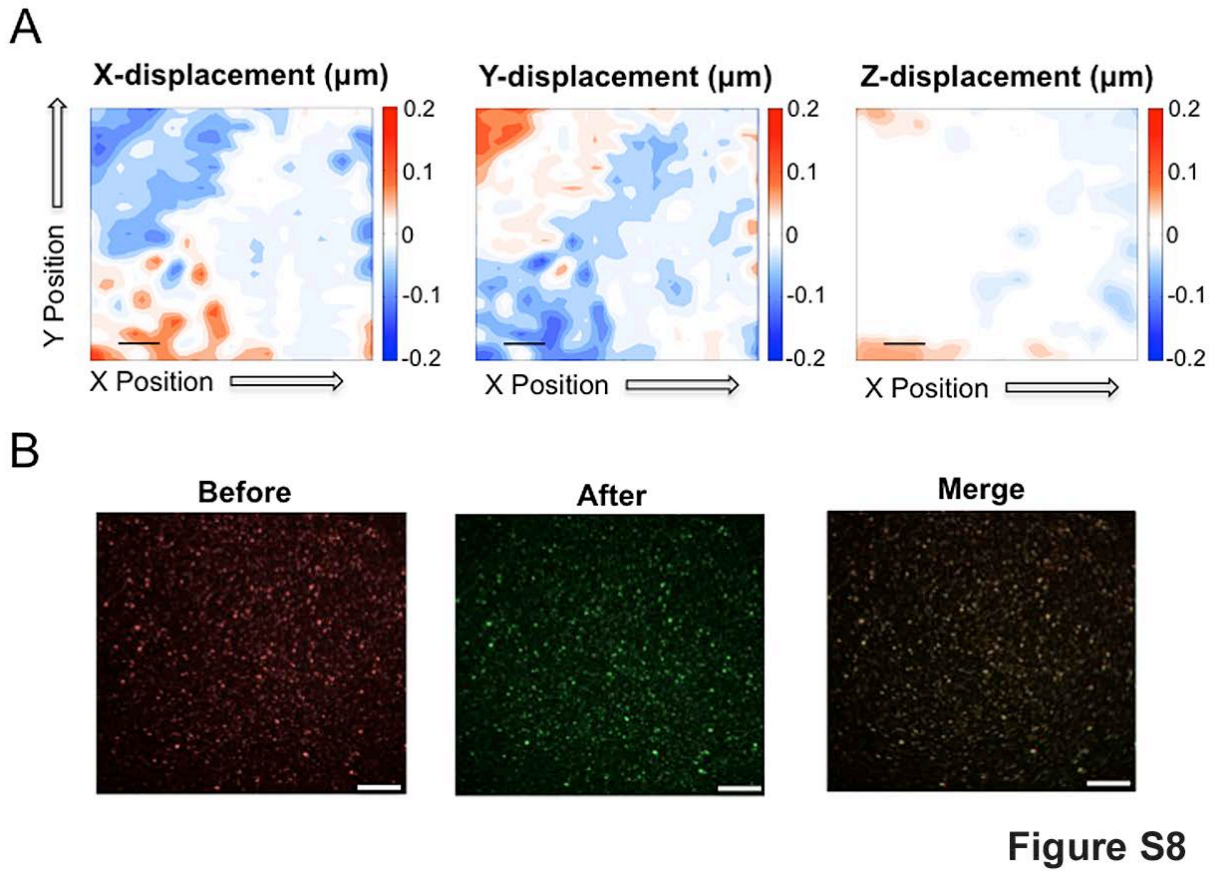

Figure S8: Matrigel networks exhibit complete elastic recovery for compressive stresses >200 Pa. (A) Three components of the displacement field measured for a Matrigel network that was subjected to a compressive pressure of 207.4 Pa. (B) Confocal images of the Matrigel networks embedded with beads before and after subjecting them to the compressive pressure. The identical images reveal the absence of any permanent matrix deformation due to the application of compressive pressure of 207.4 Pa. Scale bars: 10 μm.

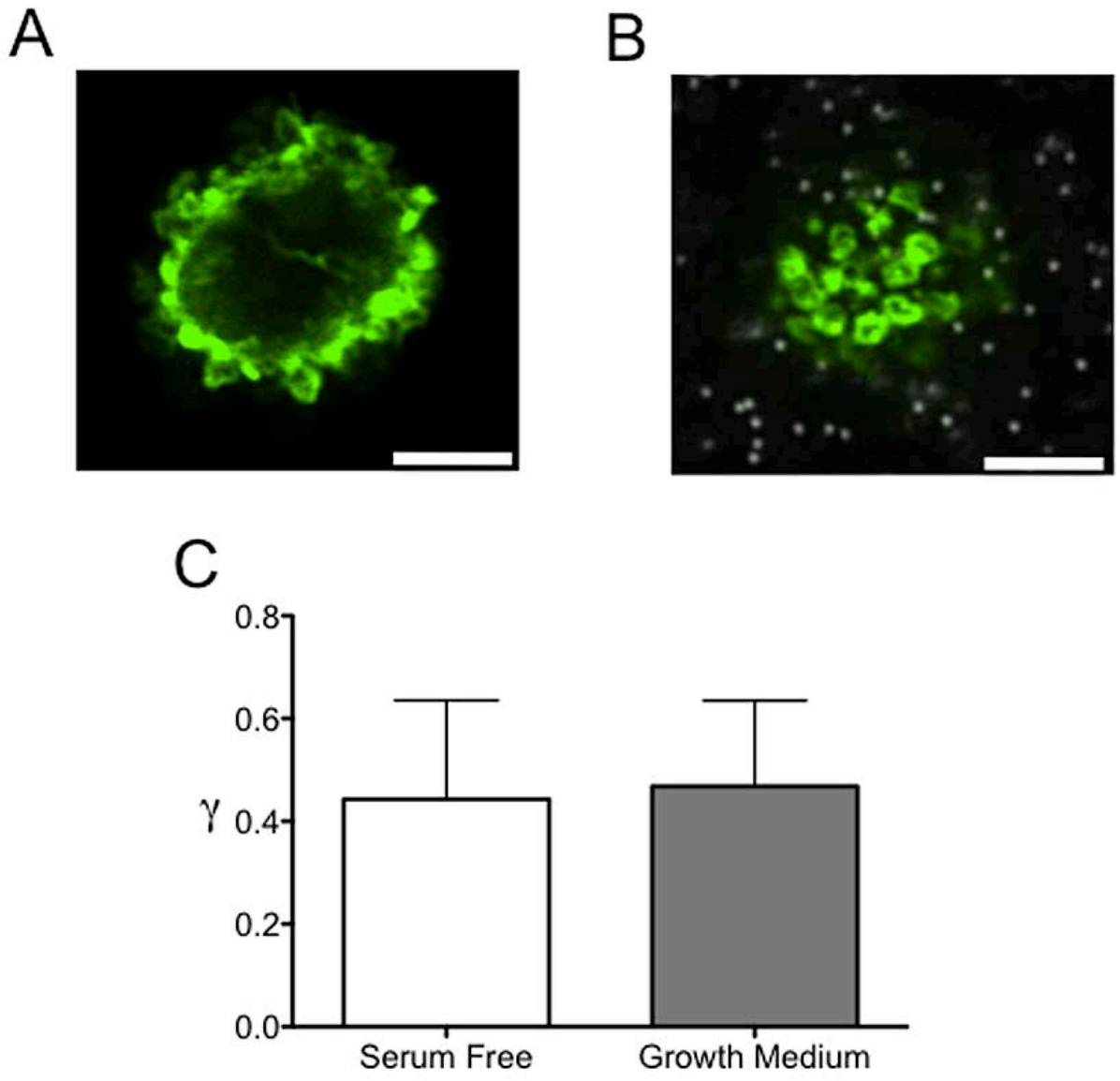

Figure S9

Figure S9: Invasion of cells in serum free conditions. The invasion of MDA-MB-231 cells in a serum free condition was analyzed for 30 μm thick Matrigels. F-actin staining shows blebbing of the invading cells as indicated by curved actin structures from the confocal section of the cell 10 μm above the leading edge (A) and at the leading edge (B). (C) The gamma values generated by the cells are comparable in both growth medium containing serum and serum free medium at $\phi_{3D} > 20°$.

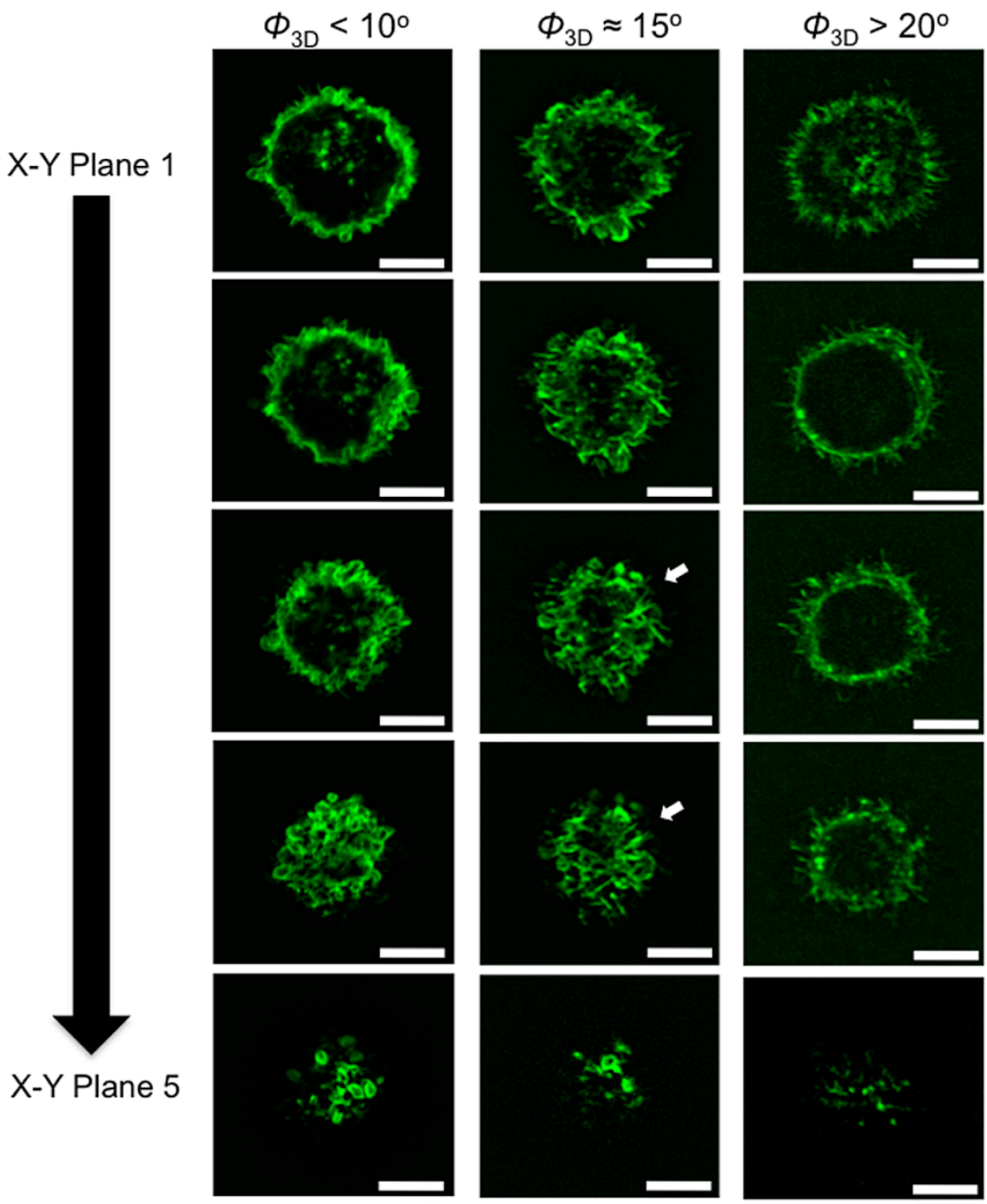

Figure S10: Morphological transition at the leading edge of the cells invading into 30 μm thick Matrigel. Cross sectional images of cells stained for F-actin at different ϕ_{3D} values. X-Y Plane 1 indicates the region 10 μm above the leading edge while X-Y Plane 5 indicates the leading edge of the invading cell. White arrows show the actin-rich protrusions. Scale bar: 10 μm.

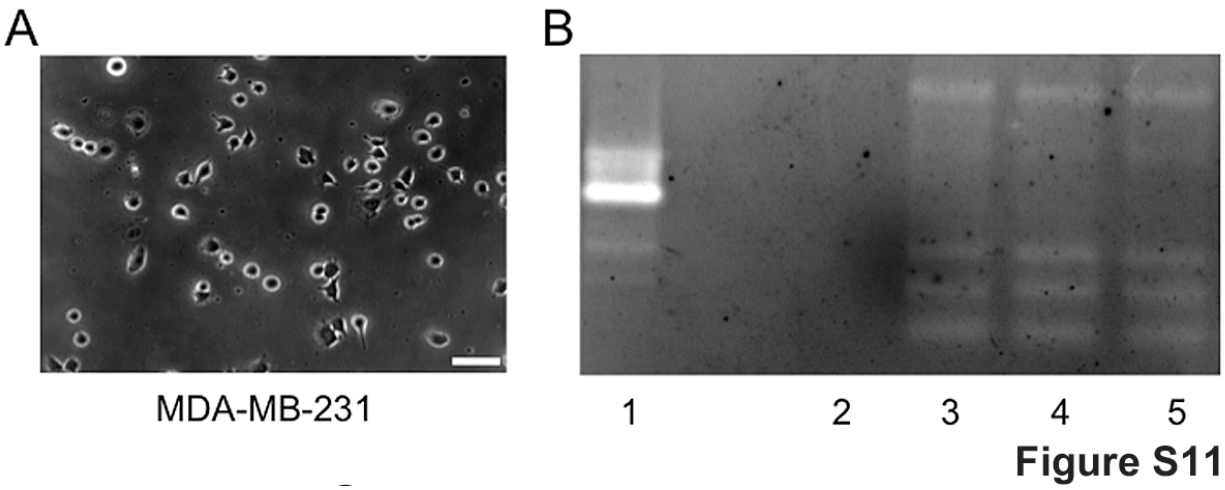

Figure S11: Secreted proteases during cell invasion using zymography. (A) Phase contrast images of MDA-MB-231 cell cultured on 30 μm thick Matrigel in Opti-MEM (OM) at an initial cell density of 10,000 cells/cm^2. (B) Gelatin zymogram for different samples. Lane 1: 0.1 μg of bovine collagenase IV containing OM collected from acellular Matrigel as a positive control. Lane 2: OM incubated with Matrigel as a negative control. Lane 3: OM collected during cell invasion (ϕ_{3D} > 20°). Lane 4: OM collected during cell invasion incubated with 1 mM APMA dissolved in 80 mM NaOH to activate proenzymes. Lane 5: OM collected during cell invasion incubated with 80 mM NaOH.

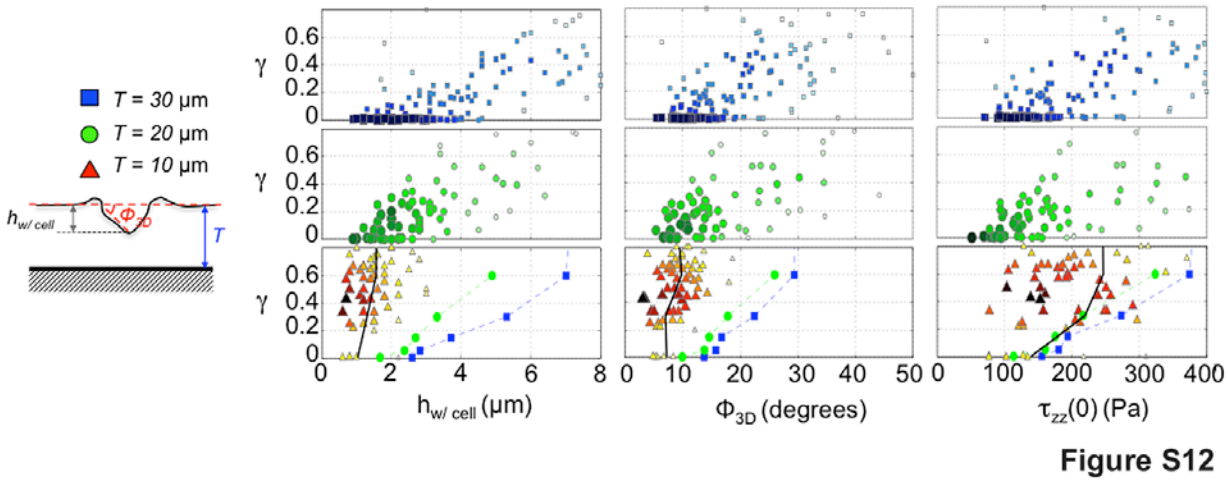

Figure S12

Figure S12: Establishing the dependence of γ on $h_{w/cell}$ ϕ_{3D}, and τ_{zz}. Scatter plots showing the extent of permanent matrix deformation caused by the invading cells, γ, in Matrigels of varying thickness, *T*, and represented as a function of different parameters listed below. In all panels, each symbol corresponds to one cell. The size and color of the symbols is proportional to the density of data points such that large, dark symbols indicate highly frequent observations. Left column: γ versus cell penetration $h_{w/cell}$ (units μm). Center column: γ versus cell indentation angle ϕ_{3D}. Right column: γ versus maximum compressive traction stress, $\tau_{zz}(0)$ (units Pa). Top row (blue squares): T = 30 μm; middle row (green circles): T = 20 μm; bottom row (red triangles): T = 10 μm. The line plots in each panel of the bottom row represent the median values of $h_{w/cell}$ (left column), ϕ_{3D} (center column) or $\tau_{zz}(0)$ (right column) corresponding to each value of γ for the three Matrigel thicknesses (blue line: T = 30 μm, green line: T = 20 μm, black line: T = 10 μm) to indicate collapse or lack of collapse of the data obtained for different T values.

Supporting References

1. Dimitriadis, E. K., F. Horkay, J. Maresca, B. Kachar, and R. S. Chadwick. 2002. Determination of elastic moduli of thin layers of soft material using the atomic force microscope. Biophys J 82:2798-2810.
2. del Alamo, J. M., R.; Alvarez-Gonzalez, B; Alonso-Latorre, B; Firtel, RA; Lasheras, JC. in press. Three-Dimensional Quantification of Cellular Traction Forces and Mechanosensing of Thin Substrata by Fourier Traction Force Microscopy. PLoS One.
3. Troeberg, L., and H. Nagase. 2003. Measurement of matrix metalloproteinase activities in the medium of cultured synoviocytes using zymography. Methods Mol Biol 225:77-87.